

SAR Image Despeckling Algorithms using Stochastic Distances and Nonlocal Means

Leonardo Torres and Alejandro C. Frery

Laboratório de Computação Científica e Análise Numérica – LaCCAN

Universidade Federal de Alagoas – UFAL

57072-970, Maceió, AL – Brazil

Email: {ljmtorres, acfrery}@gmail.com

Abstract—This paper presents two approaches for filter design based on stochastic distances for intensity speckle reduction. A window is defined around each pixel, overlapping samples are compared and only those which pass a goodness-of-fit test are used to compute the filtered value. The tests stem from stochastic divergences within the Information Theory framework. The technique is applied to intensity Synthetic Aperture Radar (SAR) data with homogeneous regions using the Gamma model. The first approach uses a Nagao-Matsuyama-type procedure for setting the overlapping samples, and the second uses the nonlocal method. The proposals are compared with the Improved Sigma filter and with anisotropic diffusion for speckled data (SRAD) using a protocol based on Monte Carlo simulation. Among the criteria used to quantify the quality of filters, we employ the equivalent number of looks, and line and edge preservation. Moreover, we also assessed the filters by the Universal Image Quality Index and by the Pearson correlation between edges. Applications to real images are also discussed. The proposed methods show good results.

Index Terms—Despeckling; Information Theory; Nonlocal means; SAR data; Stochastic Distances.

I. INTRODUCTION

Synthetic Aperture Radar (SAR) data are generated by a system of coherent illumination and are affected by the interference coherent of the signal. It is known that these data incorporate a granular noise, known as speckle noise, that degrades its quality. This noise is also present in the laser, ultrasound-B, and sonar imagery [1].

The speckle phenomenon in SAR data hinders the interpretation of these data and reduces the accuracy of segmentation, classification and analysis of objects (targets) contained within the image. Therefore, reducing the noise effect is an important task, and multilook processing is often used for this purpose in single-channel data.

Lee et al. [2], [3] proposed techniques for speckle reduction based on the multiplicative noise model using the minimum mean-square error (MMSE) criterion. Lee et al. [4] proposed a methodology for selecting neighboring pixels with similar scattering characteristics, known as Refined Lee filter. The Improved Sigma filter [5] is an improvement of the previous proposals, where an undesired blurring was solved by redefining the sigma range based on the speckle probability density functions.

Çetin and Karl [6] presented a technique for image filtering based on regularized image reconstruction. This approach

employs a tomographic model which allows the incorporation of prior information about, among other features, the sensor. The resulting images have many desirable properties, reduced speckled among them. Our approach deals with data already produced and, thus, does not require interfering in the processing protocol of the data.

Osher et al. [7] presented a novel iterative regularization method for inverse problems based on the use of Bregman distances using a total variation denoising technique tailored to additive noise. The authors also propose a generalization for multiplicative noise, but no results with this kind of contamination are shown. The main contributions were the rigorous convergence results and effective stopping criteria for the general procedure, that provides information on how to obtain an approximation of the noise-free image intensity.

More recent proposals are based on nonlocal (NL) means method originally proposed by Buades et al. [8] which is based on the redundancy of neighboring patches. The noise-free estimated value of a pixel is defined as a weighted mean of pixels in a certain region. Under the Additive White Gaussian Noise (AWGN) assumption, these weights are calculated using Euclidean distances to measure the similarity between a central region patch and neighboring patches in a search window. However, the speckle noise is not well described by a Gaussian distribution requiring, thus, changes in the model.

Deledalle et al. [9] analyzed several similarity criteria for data which depart from the Gaussian assumption, viz., the Gamma and Poisson noises. In [10] the same authors extended the NL-means method to speckled imagery using statistical inference in an iterative procedure. The authors derived the weights using the likelihood function of Gaussian and square root of Gamma (termed “Nakagami-Rayleigh”) noises. In [11], the authors proposed the use of a nonlocal approach to estimate jointly reflectivity, phase difference and coherence from a pair of co-registered single-look complex SAR images.

Coupé et al. [12] also used a logarithmic transformation and assume zero-mean Gaussian noise to propose the Optimized Bayesian NL-means with block selection (OBNLM). The OBNLM filter is an optimized version of the filter proposed by Kervrann et al. [13] which employs a new distance for comparing patches and then selecting the most similar pixels.

Parrilli et al. [14] presented a nonlocal technique based on Block-Matching 3D for SAR images (SAR-BM3D) inspired

by the algorithm presented in [15] for AWGN denoising. The SAR-BM3D filter has two steps: first, the algorithm estimates the noise-free image, and the second step, the algorithm filters anew using the more reliable statistics computed on the basic estimate to improve the filter performance.

Statistical analysis is essential for dealing with speckled data. Different statistical distributions are proposed in the literature to describe speckle data. It provides comprehensive support for developing procedures for interpreting the data efficiently, and to simulate plausible images. In this paper we use the Gamma distribution to describe the speckle noise, and a constant to characterize the ground truth [?].

This paper presents two approaches for speckle noise filtering: the first, a local nonlinear procedure, and the second, an adaptive nonlinear extension of the NL-means algorithm introduced by Buades et al. [8]. The first approach [16], [17], termed Stochastic Distances Nagao-Matsuyama (SDNM) filter, uses the neighborhoods defined by Nagao and Matsuyama [18] around each pixel; samples are compared and only those which pass a goodness-of-fit test based on stochastic distances between distributions. The test is based on a stochastic distance whose good statistical properties stem from the Information Theory framework. The improvement of previous works, the second approach, we called Stochastic Distance Nonlocal Means (SDNLM). An improvement of this latest proposal applied to PolSAR data is found in [19].

The paper is organized as follows: Section II presents the statistical modeling used to describe speckle data. In Section III samples are compared and only those which pass a goodness-of-fit test based on stochastic distances between distributions. Section IV presents the metrics for assessing the quality of the filtered images. Sections V and VI present the results and conclusions, respectively.

II. THE MULTIPLICATIVE MODEL

According to [1], the multiplicative model can be used to describe SAR data. This model asserts that the intensity observed in each pixel is the outcome of the random variable Z which, in turn, is the product of two independent non-negative random variables: X , that characterizes the mean radar reflectivity or radar cross section; and Y , which models speckle noise. The law which describes the observed intensity $Z = XY$ is completely specified by the distributions proposed for X and Y .

This paper assumes locally homogeneous intensity images, so the constant scale parameter $X = \lambda > 0$ defines the backscatter, and the unitary-mean Gamma distribution models the multilook speckle noise. Thus, it follows that $Z \sim \Gamma(L, L/\lambda)$ and its density is

$$f_Z(z; L, \lambda) = \frac{L^L}{\lambda^L \Gamma(L)} z^{L-1} \exp\left\{-\frac{Lz}{\lambda}\right\}, \quad z > 0, \quad (1)$$

where Γ stands for the Gamma function and $L \geq 1$ is the equivalent number of looks. We describe different levels of heterogeneity by allowing the number of looks L to vary locally. In a similar way, Sølbo & Eltoft [20] assume a Gamma

distribution in a wavelet-based speckle reduction procedure, and they locally estimate all the parameters without imposing a fixed number of looks (which they call “degree of heterogeneity”) for the whole image. These authors use a large 33×33 neighborhood to estimate this parameter, whereas we employ small windows.

The likelihood of $\mathbf{z} = (z_1, z_2, \dots, z_n)$, a random sample of size n from the $\text{Gamma}(L, L/\lambda)$ law, is given by

$$\mathcal{L}(L, \lambda; \mathbf{z}) = \left(\frac{L^L}{\lambda^L \Gamma(L)}\right)^n \prod_{j=1}^n z_j^{L-1} \exp\left\{-\frac{Lz_j}{\lambda}\right\}. \quad (2)$$

Thus, the maximum likelihood estimator for (L, λ) , namely $(\hat{L}, \hat{\lambda})$, is given by $\hat{\lambda} = n^{-1} \sum_{j=1}^n z_j$ and by the solution of

$$\ln \hat{L} - \psi^0(\hat{L}) - \ln \frac{1}{n} \sum_{j=1}^n z_j + \frac{1}{n} \sum_{j=1}^n \ln z_j = 0, \quad (3)$$

where ψ^0 is the digamma function [17].

III. STOCHASTIC DISTANCES FILTER

A. Neighborhood of the first approach

The first filter, initially proposed in [16], [17], is local and nonlinear. It is based on stochastic distances and tests between distributions [21], obtained from the class of (h, ϕ) -divergences. The proposal employs the neighborhoods defined by Nagao and Matsuyama [18].

Each filtered pixel has a 5×5 neighborhood, within which nine areas are defined and treated as different samples. Denote $\hat{\theta}_1$ the estimated parameter in the central 3×3 neighborhood, and $(\hat{\theta}_2, \dots, \hat{\theta}_9)$ the estimated parameters in the eight remaining areas. To account for possible departures from the homogeneous model, we estimate $\hat{\theta}_i = (L_i, \lambda_i)$, $i = \{1, \dots, 9\}$ by maximum likelihood. The filtered value is the result of averaging the central patch with those that pass the goodness-of-fit test at a certain level of confidence stipulated by the user.

B. Neighborhood of the second approach

In this approach the neighborhoods of the central pixel and of its surrounding pixels are of the same size: 3×3 pixels. The central patch, with center pixel z_1 , is thus compared with 24 neighboring patches, whose center pixels are z_i , $i = 2, \dots, 25$, as illustrated in Figure 1. The estimate of the noise-free observation at z_1 is a weighted sum of the observations at z_2, \dots, z_{25} , being each weight a function of the p -value ($p(1, i)$) observed in the statistical test of same distribution between two Gamma laws:

$$w(1, i) = \begin{cases} 1 & \text{if } p(1, i) \geq \eta, \\ \frac{2}{\eta} p(1, i) - 1 & \text{if } \frac{\eta}{2} < p(1, i) < \eta, \\ 0 & \text{otherwise,} \end{cases} \quad (4)$$

where η is the confidence of the test, chosen by the user. This function is illustrated in Figure 2. In this way we employ a soft threshold instead of an accept-reject decision. This allows the use of more evidence than with a binary decision.

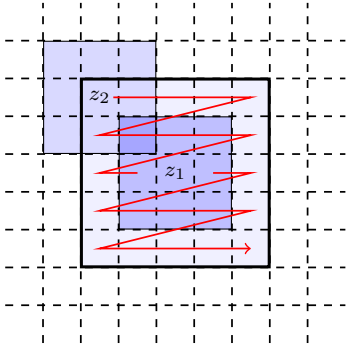


Fig. 1. Central pixel z_1 and its neighboring z_i , $i = \{2, \dots, 25\}$ with 3×3 pixels patches.

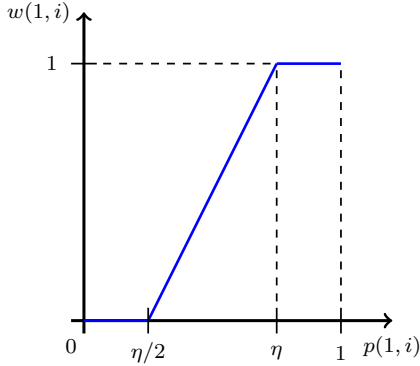


Fig. 2. Weight function for every pair of patches $(1, i)$, $2 \leq i \leq 25$.

In this way, this proposal employs those pixels whose observations are not rejected by a test of strong isotropy with respect to the central value.

C. Stochastic Distances Filter

The proposals are based on the use of stochastic distances on small areas within the filtering window. Consider Z_1 and Z_i random variables defined on the same probability space, characterized by the densities $f_{Z_1}(z_1; \theta_1)$ and $f_{Z_i}(z_i; \theta_i)$, respectively, where θ_1 and θ_i are parameters. Assuming that both densities have the same support $I \subset \mathbb{R}$, the (h, ϕ) -divergence between the distributions is given by

$$D_{\phi}^h(Z_1, Z_i) = h\left(\int_{x \in I} \phi\left(\frac{f_{Z_1}(x; \theta_1)}{f_{Z_i}(x; \theta_i)}\right) f_{Z_i}(x; \theta_i) dx\right), \quad (5)$$

where $h: (0, \infty) \rightarrow [0, \infty)$ is a strictly increasing function with $h(0) = 0$ and $h'(x) > 0$; and $\phi: (0, \infty) \rightarrow [0, \infty)$ is a convex function for all $x \in \mathbb{R}$. Choices of the functions h and ϕ result in several divergences.

Divergences sometimes do not obey the requirements to be considered distances. A simple solution is to define a new measure, the distance d_{ϕ}^h , given by

$$d_{\phi}^h(Z_1, Z_i) = \frac{D_{\phi}^h(Z_1, Z_i) + D_{\phi}^h(Z_i, Z_1)}{2}. \quad (6)$$

Distances, in turn, can be conveniently scaled in order to present good statistical properties that make them test statistics [21]:

$$S_{\phi}^h(\hat{\theta}_1, \hat{\theta}_i) = \frac{2mnk}{m+n} d_{\phi}^h(\hat{\theta}_1, \hat{\theta}_i), \quad (7)$$

where $\hat{\theta}_1$ e $\hat{\theta}_i$ are maximum likelihood estimators based on samples size m and n , respectively, and $k = (h'(0)\phi''(1))^{-1}$. The null hypothesis $\theta_1 = \theta_i$ is rejected at a level η , if $\Pr(S_{\phi}^h > s) \leq \eta$, where s is the observed value. Under mild conditions S_{ϕ}^h is χ_M^2 asymptotically distributed, being M the dimension of θ_1 , the test is well defined. Details can be seen in the work by Salicrú et al. [22]. Several statistical tests were derived (Hellinger, Bhattacharyya, Triangular, χ^2 , and Rényi of order β), and the one with the best computational performance was the one based on the Kullback-Leibler divergence:

$$S_{KL} = \frac{mn(\hat{L}_1 + \hat{L}_i)}{m+n} \left(\frac{\hat{\lambda}_1^2 + \hat{\lambda}_i^2}{2\hat{\lambda}_1\hat{\lambda}_i} - 1 \right). \quad (8)$$

The filtering procedure consists in checking which regions can be considered as coming from the same distribution that produced the data which comprises the central block. The sets which are not rejected are used to compute a local mean. If all the sets are rejected, the filtered value is updated with the average on the 3×3 neighborhood around the filtered pixel.

IV. IMAGE QUALITY ASSESSMENT

Image quality assessment in general, and filter performance evaluation in particular, are hard tasks [23]. Moschetti et al [24] discussed the need of making a Monte Carlo study when assessing the performance of image filters. They proposed a protocol which consists of using a phantom image (see Figure 3(a)) corrupted by speckle noise (see Figure 3(b)). The experiment consists of simulating corrupted images as matrices of independent samples of some distribution with different parameters. Every simulated image is subjected to filters, and the results are compared (see Figures 3(c) to 3(f)).

Among the criteria used to quantify the quality of the filters, we employ [24]:

- **Equivalent Number of Looks:** in intensity imagery and homogeneous areas, it can be estimated by $ENL = (\bar{z}/\hat{\sigma}_Z)^2$, i.e., the square of the reciprocal of the coefficient of variation. In this case, the bigger the better.
- **Line Contrast:** the preservation of a line of one pixel of width will be assessed by computing three means: in the coordinates of the original line (x_{ℓ}) and in two lines around it (x_{ℓ_1} and x_{ℓ_2}). The contrast is then defined as $2x_{\ell} - (x_{\ell_1} + x_{\ell_2})$, and compared with the contrast in the phantom. The best values are the smallest.
- **Edge Preserving:** it is measured by means of the edge gradient (the absolute difference of the means of strip around edges) and variance (same as the former but using variances instead of means). The best values are the smallest.

A “good” technique must combat speckle and, at the same time, preserve details as well as relevant information.

Furthermore, we also assessed the filters by the universal image quality index [23], the correlation measure β_{ρ} and the BRISQUE model [25] on real images. The universal image quality index is defined by

$$Q = \frac{s_{xy}}{s_x s_y} \frac{2\bar{x}\bar{y}}{\bar{x}^2 + \bar{y}^2} \frac{2s_x s_y}{s_x^2 + s_y^2}, \quad (9)$$

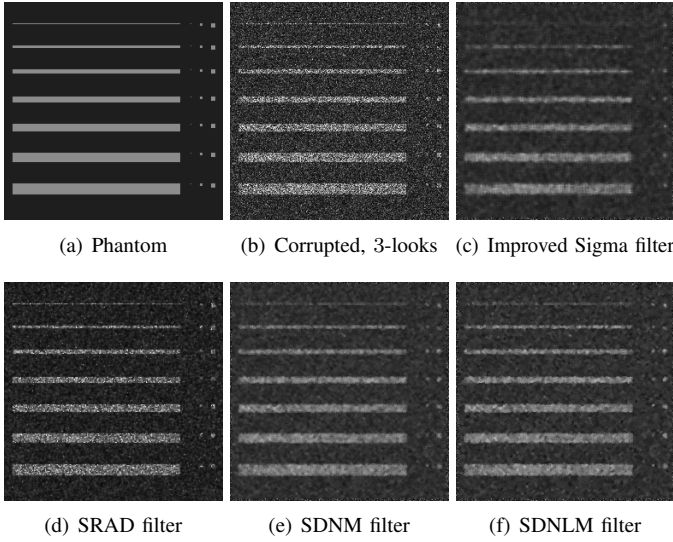


Fig. 3. Lee's Protocol phantom, speckled data and filtered images.

where s_j^2 and $\bar{\bullet}$ denote the sample variance and mean, respectively. The range of Q is $[-1, 1]$, being 1 the best value. The quantity

$$\beta_\rho = \frac{\sum_{j=1}^n (x_j - \bar{x})(y_j - \bar{y})}{\sqrt{\sum_{j=1}^n (x_j - \bar{x})^2 \sum_{j=1}^n (y_j - \bar{y})^2}}, \quad (10)$$

is a correlation measure is between the Laplacians of images X and Y , where \bullet_j and $\bar{\bullet}$ denote the gradient values of the j th pixel and mean of the images $\nabla^2 X$ and $\nabla^2 Y$, respectively. The range of β_ρ is $[-1, 1]$, being 1 perfect correlation.

The BRISQUE is a model that operates in the spatial domain and requires no-reference image. This image quality evaluator does not compute specific distortions such as ringing, blurring, blocking, or aliasing, but quantifies possible losses of “naturalness” in the image. This approach is based on the principle that natural images possess certain regular statistical properties that are measurably modified by the presence of distortions. No transformation to another coordinate frame (DFT, DCT, wavelets, etc) is required, distinguishing it from previous blind/no-reference approaches. The BRISQUE is defined for scalar-valued images and it ranges in the $[0, 100]$ interval, and smaller values indicate better results.

Figure 4 shows a block diagram of the assessment method for the first proposal.

V. RESULTS AND ANALYSIS

The proposals were compared with the Improved Sigma filter [5] and the SRAD (Speckle Reduction Anisotropic Diffusion) filter proposed by Yu and Acton [26], specifically designed for combating speckle. The Improved Sigma filter was applied in windows of sides 5. The SRAD filter used a window of side 5, and diffusion threshold $q_0 = 1/2$. The tests of the stochastic distances filters were performed at the 90% level of significance.

Table I presents the three situations that were simulated. These parameters describe situations commonly found when analyzing SAR imagery in homogeneous regions.

TABLE I
SIMULATED SITUATIONS WITH THE GAMMA($L, L/\lambda$) DISTRIBUTION.

| Situation ID | L | λ_ℓ | Background mean |
|--------------|-----|----------------|-----------------|
| #1 | 1 | 200 | 20 |
| #2 | 3 | 195 | 55 |
| #3 | 4 | 150 | 30 |

The results obtained in one hundred independent replications are summarized in Table II: the mean and the standard deviation (in parenthesis) of each measure are shown in each situation. Only the results of applying the filter once are presented, for $L = \{1, 3, 4\}$ looks following the Table I, and the best results are highlighted in bold.

As expected, the Improved Sigma filter (denoted as Lee) is the one which provides the strongest speckle reduction as measured by the equivalent number of looks (ENL). This filter was designed with that purpose in mind. When it comes to measures of detail preservation, our proposal is the winner.

Not every aforementioned quality measure can be applied to real data, unless the ground truth is known. One of the quality measures that can be used in this case is the BRISQUE index [25].

Figure 5 presents the results of applying the filters to an image obtained by the Danish EMISAR L-band fully polarimetric sensor over agricultural fields in Foulum, Denmark. The original 250×350 pixels image of the HH intensity band is shown in Fig. 5(a), its filtered versions by the Improved Sigma, SRAD, SDNM and SDNLM filters are presented in Figs. 5(b), 5(c), 5(d) and 5(e), respectively. Figure 5(f) presents the values of row 300.

Table III presents the observed BRISQUE index and equivalent number of looks on the real image. It is noticeable that the proposed technique produces better results than the Improved Sigma, SRAD and SDNM filters regarding the BRISQUE index by a significant margin. As expected, it provides a smaller increase in the equivalent number of looks, especially in the second image, which exhibits more spatial variability and thus leads to a more conservative filter.

TABLE III
IMAGE QUALITY INDEXES IN THE REAL SAR IMAGE.

| Filtered Versions | BRISQUE Index | ENL |
|-------------------|---------------|--------------|
| Improved Sigma | 49.239 | 4.581 |
| SRAD | 39.235 | 3.101 |
| SDNM | 39.164 | 4.661 |
| SDNLM | 37.384 | 4.539 |

VI. CONCLUSIONS

This paper presented an assessment of the filter based on stochastic distances for speckle noise reduction. The proposal

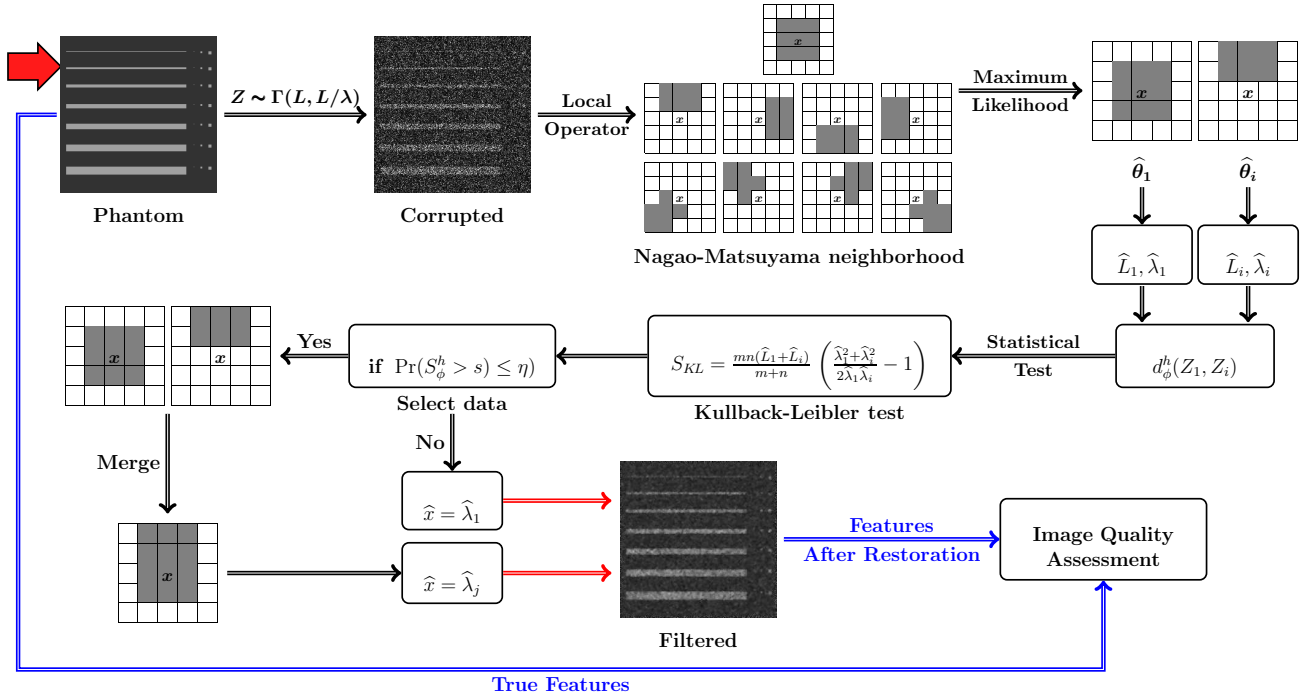


Fig. 4. Block diagram for assessment of the first proposed technique.

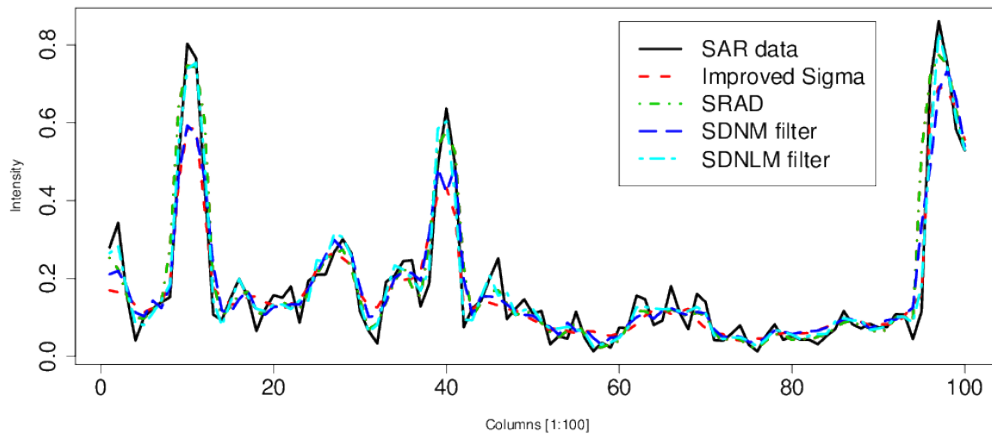
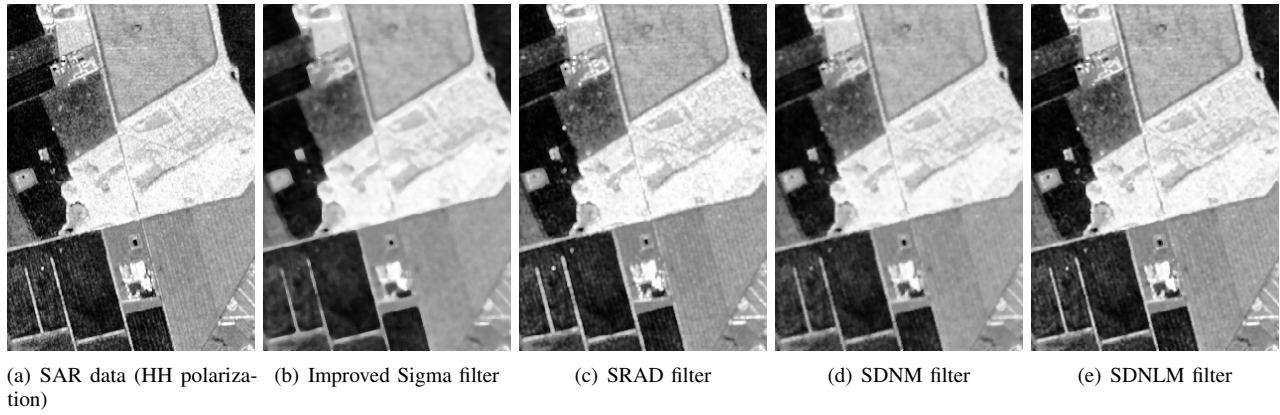
TABLE II
STATISTICS OF THE METRICS OF SIMULATED IMAGES: 100 REPLICATIONS WITH 1-ITERATION.

| Filtered Versions | SAR Measures | | | | Q Index | β_p Index |
|-------------------|---------------|------------|---------------|------------------------|-----------------------|---|
| | ENL | Line Cont. | Edge Grad. | Edge Var. | | |
| Improved Sigma #1 | 14.375 | (2.034) | 1.724 (0.032) | 74.806 (10.065) | 2.117 | (1.426) 0.149 (0.002) 0.747 (0.005) |
| SRAD #1 | 1.009 | (0.144) | 1.798 (0.027) | 84.217 (8.066) | 2.533 (1.108) | 0.001 (0.000) 0.793 (0.007) |
| SDNM #1 | 13.391 | (1.333) | 1.566 (0.035) | 61.975 | (6.900) 4.533 (1.234) | 0.220 (0.002) 0.812 (0.009) |
| SDNLM #1 | 12.054 | (3.393) | 1.522 | (0.041) 64.531 (6.789) | 5.020 (1.256) | 0.226 (0.002) 0.822 (0.008) |
| Improved Sigma #2 | 54.467 | (7.226) | 1.495 (0.029) | 62.709 (5.038) | 6.772 (1.492) | 0.198 (0.002) 0.784 (0.006) |
| SRAD #2 | 3.158 | (0.421) | 1.639 (0.042) | 72.925 (5.583) | 6.444 (1.250) | 0.001 (0.000) 0.811 (0.011) |
| SDNM #2 | 40.234 | (3.978) | 1.393 (0.041) | 61.975 | (6.900) 6.736 (1.321) | 0.235 (0.002) 0.840 (0.010) |
| SDNLM #2 | 43.495 | (6.514) | 1.361 | (0.060) 64.531 (6.789) | 5.899 | (1.644) 0.243 (0.001) 0.845 (0.010) |
| Improved Sigma #3 | 90.238 | (10.939) | 1.401 (0.024) | 47.230 (6.051) | 8.315 (1.728) | 0.218 (0.001) 0.845 (0.002) |
| SRAD #3 | 4.765 | (0.850) | 1.511 (0.046) | 63.068 (8.751) | 3.528 | (0.875) 0.001 (0.000) 0.863 (0.005) |
| SDNM #3 | 65.678 | (7.451) | 1.293 (0.037) | 37.255 | (4.928) 6.053 (1.619) | 0.248 (0.001) 0.883 (0.003) |
| SDNLM #3 | 66.485 | (19.580) | 1.207 | (0.063) 47.866 (3.581) | 4.765 (1.518) | 0.262 (0.001) 0.899 (0.007) |

was compared with the Improved Sigma filter and other more sophisticated filters, using a protocol based on Monte Carlo experiences and real images. Moreover, the β_p , Q index and BRISQUE model were used to assert the proposal. The proposed filter outperforms the Improved Sigma filter in five out of six quality measures. Other significance levels will be tested, along with different points of the parameter space of the simulation in order to have a more complete assessment of the proposal.

REFERENCES

- [1] J. W. Goodman, "Some fundamental properties of speckle," *Journal of the Optical Society of America*, vol. 66, no. 11, pp. 1145–1150, 1976.
- [2] J.-S. Lee, M. R. Grunes, and G. de Grandi, "Polarimetric SAR speckle filtering and its implication for classification," *IEEE Transactions on Geoscience and Remote Sensing*, vol. 37, no. 5, pp. 2363–2373, 1999.
- [3] J.-S. Lee, M. R. Grunes, and S. A. Mango, "Speckle reduction in multipolarization, multifrequency SAR imagery," *IEEE Transactions on Geoscience and Remote Sensing*, vol. 29, no. 4, pp. 535–544, 1991.
- [4] J.-S. Lee, M. R. Grunes, D. L. Schuler, E. Pottier, and L. Ferro-Famil, "Scattering-model-based speckle filtering of Polarimetric SAR data," *IEEE Transactions on Geoscience and Remote Sensing*, vol. 44, no. 1, pp. 176–187, 2006.
- [5] J.-S. Lee, J.-H. Wen, T. L. Ainsworth, K.-S. Chen, and A. J. Chen, "Improved sigma filter for speckle filtering of SAR Imagery," *IEEE Transactions on Geoscience and Remote Sensing*, vol. 47, no. 1, pp. 202–213, 2009.
- [6] M. Çetin and W. C. Karl, "Feature-enhanced synthetic aperture radar image formation based on nonquadratic regularization," *IEEE Transactions on Image Processing*, vol. 10, no. 4, pp. 623–631, 2001.
- [7] S. Osher, M. Burger, D. Goldfarb, J. Xu, and W. Yin, "An iterated regu-



(f) 1-D analysis on row 300

Fig. 5. Real data, filtered versions and 1-D analysis of row 300.

- larization method for total variation-based image restoration,” *Multiscale Modeling & Simulation*, vol. 4, no. 2, pp. 460–489, 2005.
- [8] A. Buades, B. Coll, and J. M. Morel, “A review of image denoising algorithms, with a new one,” *Multiscale Modeling & Simulation*, vol. 4, no. 2, pp. 490–530, 2005.
- [9] C.-A. Deledalle, F. Tupin, and L. Denis, “Patch similarity under non gaussian noise,” in *IEEE International Conference on Image Processing (ICIP)*, 2011, pp. 1845–1848.
- [10] C.-A. Deledalle, L. Denis, and F. Tupin, “Iterative weighted maximum likelihood denoising with probabilistic patch-based weights,” *IEEE Transactions on Image Processing*, vol. 18, no. 2, pp. 2661–2672, 2009.
- [11] C.-A. Deledalle, F. Tupin, and L. Denis, “A non-local approach for SAR and interferometric SAR denoising,” in *IEEE International Geoscience and Remote Sensing Symposium (IGARSS)*, Honolulu, 2010, pp. 714–717.
- [12] P. Coupé, P. Hellier, C. Kervrann, and C. Barillot, “Nonlocal means-based speckle filtering for ultrasound images,” *IEEE Transactions Image Processing*, vol. 18, no. 10, pp. 2221–2229, 2009.
- [13] C. Kervrann, J. Boulanger, and P. Coupé, “Bayesian non-local means filter, image redundancy and adaptive dictionaries for noise removal,” in *Proc. Conf. Scale-Space and Variational Meth*, Ischia, 2007, pp. 520–532.
- [14] S. Parrilli, M. Poderico, C. V. Angelino, and L. Verdoliva, “A nonlocal SAR image denoising algorithm based on l1mmse wavelet shrinkage,” *IEEE Transactions on Geoscience and Remote Sensing*, vol. 50, no. 2, pp. 606–616, 2012.
- [15] K. Dabov, A. Foi, V. Katkovnik, and K. Egiazarian, “Image denoising by sparse 3-d transform-domain collaborative filtering,” *IEEE Transactions on Image Processing*, vol. 18, no. 8, pp. 2080–2095, 2007.
- [16] L. Torres, T. Cavalcante, and A. C. Frery, “A new algorithm of speckle filtering using stochastic distances,” in *IEEE International Geoscience and Remote Sensing Symposium (IGARSS)*, Munich, 2012.
- [17] L. Torres, T. Cavalcante, and A. Frery, “Speckle reduction using stochastic distances,” in *Pattern Recognition, Image Analysis, Computer Vision, and Applications*, ser. Lecture Notes in Computer Science, L. Alvarez et al., Ed., vol. 7441. Buenos Aires: Springer, 2012, pp. 632–639.
- [18] M. Nagao and T. Matsuyama, “Edge preserving smoothing,” *Computer Graphics and Image Processing*, vol. 9, no. 4, pp. 394–407, 1979.
- [19] L. Torres, S. J. S. Sant’Anna, C. C. Freitas, and A. C. Frery, “Speckle reduction in polarimetric SAR imagery with stochastic distances and nonlocal means,” *Pattern Recognition*, April 2013, in press.
- [20] S. Sølbo and T. Eltoft, “T-WMAP: a statistical speckle filter operating in the wavelet domain,” *International Journal of Remote Sensing*, vol. 25, no. 5, pp. 1019–1036, 2004.
- [21] A. D. C. Nascimento, R. J. Cintra, and A. C. Frery, “Hypothesis testing in speckled data with stochastic distances,” *IEEE Transactions on Geoscience and Remote Sensing*, vol. 48, no. 1, pp. 373–385, 2010.
- [22] M. Salicrú, D. Morales, M. L. Menéndez, and L. Pardo, “On the applications of divergence type measures in testing statistical hypotheses,” *Journal of Multivariate Analysis*, vol. 21, no. 2, pp. 372–391, 1994.
- [23] Z. Wang and A. C. Bovik, “A universal image quality index,” *IEEE Signal Processing Letters*, vol. 9, no. 3, pp. 81–84, 2002.
- [24] E. Moschetti, M. G. Palacio, M. Picco, O. H. Bustos, and A. C. Frery, “On the use of Lee’s protocol for speckle-reducing techniques,” *Latin American Applied Research*, vol. 36, no. 2, pp. 115–121, 2006.
- [25] A. Mittal, A. K. Moorthy, and A. C. Bovik, “No-reference image quality assessment in the spatial domain,” *IEEE Transactions on Image Processing*, vol. 21, no. 12, pp. 4695–4708, 2012.
- [26] Y. Yu and S. Acton, “Speckle reducing anisotropic diffusion,” *IEEE Transactions on Image Processing*, vol. 11, no. 11, pp. 1260–1270, 2002.